Z. Phys. Chem. **221** (2007) 527–536 / **DOI** 10.1524/zpch.2007.221.4.527

Free Volume Nanocavities in PMMA Revealed by Rotational Dephasing of Paraterphenyl in a Transient Grating Experiment

By David von Seggern, Christian Spitz*, and Ralf Menzel

Universität Potsdam, Institut für Physik, Am Neuen Palais 10, D-14469 Potsdam, Germany

(Received October 9, 2006; accepted January 29, 2007)

Transient Grating Spectroscopy / PMMA / Free Volume / Nonpolar Dopant

The excited state decay behaviour of *p*-terphenyl in cyclohexane solution and in a rigid poly(methyl methacrylate) (PMMA) film is reported as measured in a ps polarization dependent transient grating experiment. In both cases, the diffracted intensity shows a biexponential decay. The slower component is attributed to excited state lifetime. In the liquid solution, the faster decay component is described by the hydrodynamical Stokes–Einstein–Debye theory for rotational reorientation under slip boundary conditions. In the rigid matrix it is interpreted in terms of a free volume effect.

1. Introduction

The excited state decay characteristics of a solute in a given solute–solvent combination reveals valuable information about its microenvironment. An important parameter in this connection is the viscosity of the solvent as it is of substantial influence on the rotational reorientation rates of the embedded solute. As long as the solute is large compared to the solvent particle size, the interactions retarding its rotational diffusion can be visualized in the hydrodynamic Stokes–Einstein–Debye model [1–3]: the rotating solute molecule has to displace solvent particles and the resulting torque opposes the rotational motion. This model depends on shape and size of the solute and the macroscopic viscosity of the medium. In its initial form, it describes well the rotational motion of a large spherical solute in a continuous solvent under the assumption that the solvent sticks to the solute ("stick" boundary condition). The

* Corresponding author. E-mail: spitz@rz.uni-potsdam.de

model was later modified for nonspherical solute shape [4] and for the case of the solute slipping between the solvent molecules ("slip" boundary condition) [5]. However, this picture proves insufficient as soon as more complicated microscopic aspects of solute/solvent interaction come into play. Important modifications of the purely hydrodynamic model are the microfriction theory of Gierer and Wirtz [6] taking into account the discontinuous nature of the solvent and the relative sizes of solute and solvent molecules, and the "free space model" by Dote, Kivelson and Schwartz [7] that additionally refers to the free volume between the solvent molecules.

With increasing viscosity and solvent particle size molecular aspects become more and more important. Finally, an amorphous polymeric matrix can be looked upon as a rigid solvent with a high degree of internal discontinuity due to shape and size of the polymers. Solute molecules of usually considerably smaller size find highly rigid areas where they will hardly be able to carry out any motions alternating with free volume nanocavities where, depending on the ratio of solute/solvent size and on the existence of specific interactions with the polymer side chains [8–10], they will be able to move relatively unhindered [11–16].

In the present work, we compare the excited state and polarization anisotropy decay characteristics of *p*-terphenyl in a liquid cyclohexane solution to that of a rigid *p*-terphenyl doped poly(methyl methacrylate) (PMMA) film as measured in a polarization sensitive transient grating (TG) experiment [17–23].

2. Experimental

P-Terphenyl and PMMA (Degalan V26) were obtained from Aldrich and Fluka, respectively, and cyclohexane and chloroform were obtained from Merck in Uvasol® quality. The liquid samples were freshly prepared by dissolution of 20 mg *p*-terphenyl per liter cyclohexane at room temperature and enclosed in a home made quartz cell of 5 μm thickness. The *p*-terphenyl/PMMA solutions were prepared by adding *p*-terphenyl and PMMA in chloroform and stirring in an open bottle at room temperature until dissolved. The films were produced by dip coating a plane quartz substrate of 1 mm thickness into the *p*-terphenyl/PMMA solution and subsequent solvent evaporation in air providing glassy state films at room temperature. The film thickness amounted to about 3–5 μm. The maximum OD of the liquid as well as the solid samples was 0.05–0.09 at the excitation wavelength. This corresponds to concentrations of about $3.5–7.5 \times 10^{-6}$ mol/cm^3. Apparently, a certain fraction of the chromophores initially dissolved is pushed out of the films in the drying process. All experiments were carried out under room temperature.

Ground state absorption spectra were taken with a Cary 5e absorption spectrometer at a spectral resolution of 0.5 nm. Excited state absorption spec-

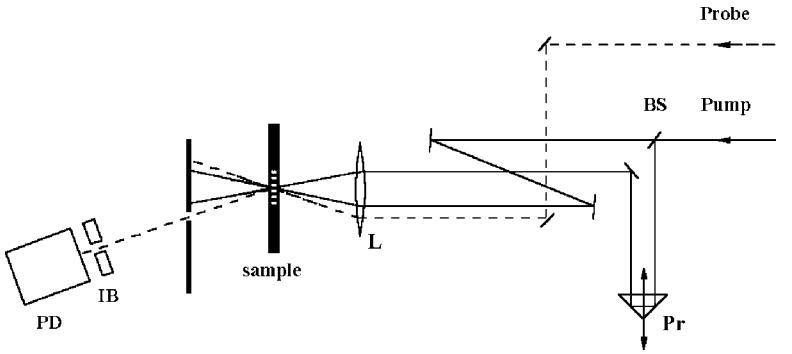

Fig. 1. Setup for the TG experiments: The pumplight is split into two at the beamsplitter BS. One of the pump beams passes a delay line Pr, allowing for an exact adjustment of the two pathlengths. Pump and probe beams are focused on the sample by a quartz lens L. After passing an iris diaphragm and an optional interference filter, the $\pm 1^{st}$ diffraction order of the probe light is detected by a photodiode and processed in a lock-in amplifier.

tra were measured with a nanosecond pump–probe apparatus equipped with a XeCl excimer laser for pump light and broad band fluorescence probe light. The system has been described previously [24–26]. For the TG experiments, we used the regeneratively amplified output of a Spectra Physics Tsunami Ti:Sa laser (Spectra Physics Spitfire, 1024 nm, 1 kHz, 750 mW, 2 ps), part of which was converted into 560 nm in a Spectra Physics OPA for the probe light. The pump light of 266 nm was obtained by THG of the remaining fundamental wave.

Figure 1 shows the experimental setup for the transient grating experiments. To produce the grating the 266 nm, 20 mJ beam is split into two at a beam splitter. One of the pump beams passes a delay line allowing a reproducable adjustment of the pathlengths of the two beams in the range of few μm. Both pump beams are focused on the sample by a quartz lens, interfering in an angle of 2° on a spot of about 1 mm in diameter. The 560 nm probe beam hits the sample at an arbitrary angle. After passing several diaphragms and an optional interference filter, the signal ($\pm 1^{st}$ diffraction order) is detected by a fast photodiode ($\tau = 200$ ps) and processed in a Perkin Elmer DSP lock-in amplifier. The two pump beams have different portions of *s* and *p* polarized light resulting in an angle of $5^\circ \pm 0.5^\circ$. Thus, the sample is modulated in a twofold way. First, the interference pattern creates a population density modulation due to the S_0–S_1 absorption. This absorptivity modulation acts as a diffraction grating for all wavelengths responding to the S_0–S_1 population redistribution, *i.e.* those belonging to the GSA (S_0–S_1) or the ESA spectrum (S_1–S_n), respectively. Second, the different portions of *s* and *p* polarization create a modulated polarization anisotropy in the sample that can be detected by a linearly polarized probe beam [17–20, 27].

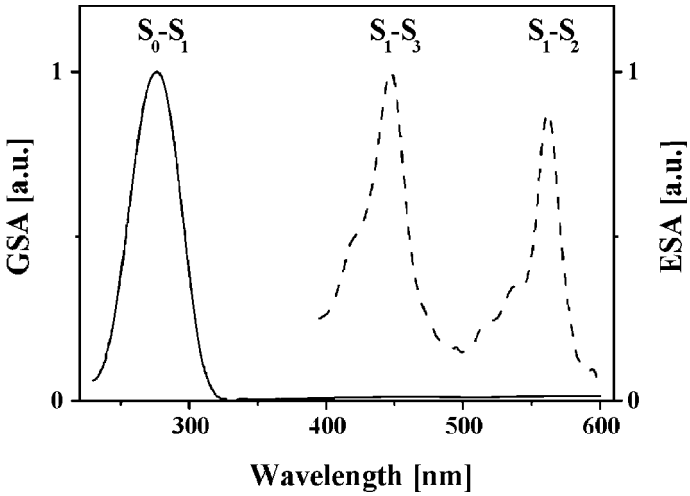

Fig. 2. Ground state (solid line) and excited state (dashed line) absorption spectra of *p*-terphenyl in cyclohexane.

The samples were mounted on an *xy* stage that could be manually moved perpendicular to the excitation beam to avoid sample degradation due to the relatively high excitation intensities. This was necessary in both cases, but in PMMA the degradation process was faster than in cyclohexane because translational diffusion of the chromophores in the rigid matrix is much more restricted.

3. Results and discussion

The ground and excited state absorption spectra of *p*-terphenyl are shown in Fig. 2. The 266 nm pump and the 560 nm probe light correspond to the S_0–S_1 and the S_1–S_2 absorption of *p*-terphenyl, respectively. Figures 3 and 4 show excited state decay curves of *p*-terphenyl in cyclohexane and in a PMMA film. The data were obtained from repeated experiments with several independently prepared solutions and films. The different liquid and solid samples provided comparable data each which were comprised in the curves presented in the figures. In all cases, each data point was recorded at a new position of the respective sample.

Because the diffraction efficiency of a transient grating is proportional to the square of the modulation depth [28], the figures show the square root of the measured diffraction signals.

The signal comprises contributions of a population grating and of a polarization grating. The decay of the polarization grating is due to excited state

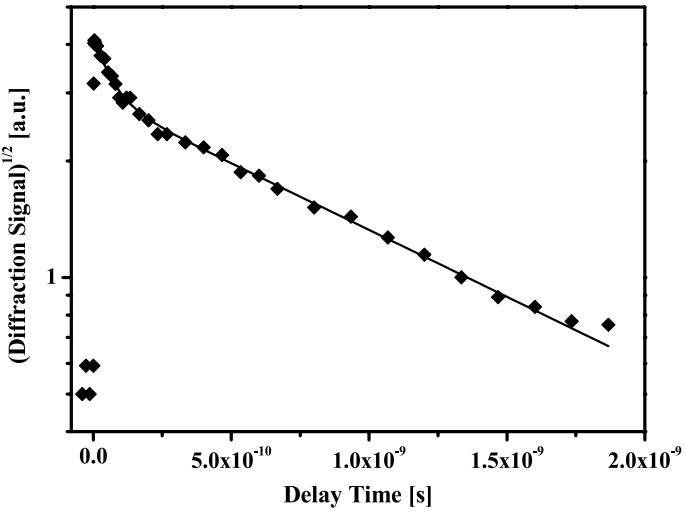

Fig. 3. Transient grating diffraction intensity in a 5 μm thick layer of *p*-terphenyl/cyclohexane solution as function of delay between pump and probe light (squares). The data points were best fitted by a double exponential function (solid line) with $\tau_{rot} = (65 \pm 12)$ ps and $\tau_{ESA} = (1258 \pm 29)$ ps. The amplitude ratio I_{rot}/I_{ESA} amounts to 0.44.

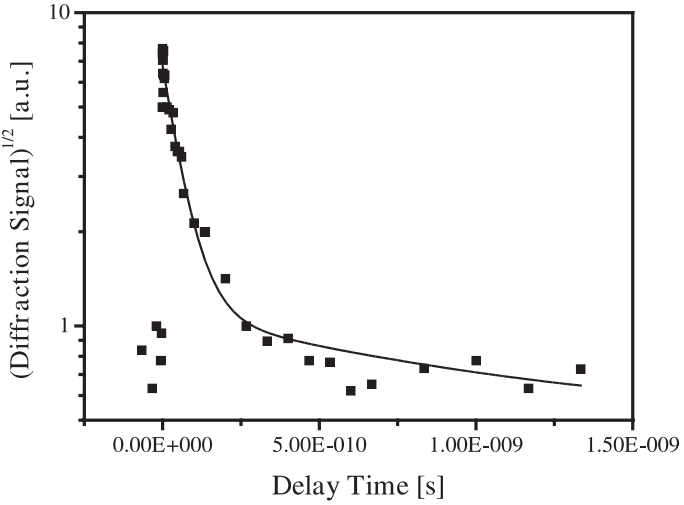

Fig. 4. Transient grating diffraction intensity in a 2 μm thick *p*-terphenyl doped PMMA film as function of delay between pump and probe light (squares). The data points were fitted by a Eq. (2) (solid line) with $\tau_{rot} = (60 \pm 7)$ ps and $\tau_{ESA} = (988 \pm 80)$ ps. The amplitude ratio I_{rot}/I_{ESA} amounts to 8.9.

relaxation and rotational reorientation. Because both processes are exponential, the polarization grating decay is described by an exponential that is the product of the two [27]:

$$I_{\mathrm{pol}}(t) = I_1 \exp[-2(t/\tau_{\mathrm{rot}} + t/\tau_{\mathrm{ESA}})] \,. \tag{1}$$

The decay of the total signal is then the sum of the decays of the polarization grating and of the excited state grating:

$$I^{1/2}(t) = I_1 \exp[-(t/\tau_{\mathrm{rot}} + t/\tau_{\mathrm{ESA}})] + I_2 \exp -(t/\tau_{\mathrm{ESA}}) \,. \tag{2}$$

This function was applied for fitting the CHx as well as the PMMA data.

In the *p*-terphenyl/cyclohexane solution, the two corresponding average lifetimes from 6 runs are $\tau_{\mathrm{rot}} = (65 \pm 12)$ ps and $\tau_{\mathrm{ESA}} = (1258 \pm 29)$ ps of the total signal.

In the *p*-terphenyl doped PMMA film, $\tau_{\mathrm{rot}} = (60 \pm 7)$ ps amounts to almost exactly the same value as in the cyclohexane solution while $\tau_{\mathrm{ESA}} = (988 \pm 80)$ ps is reduced for about 20%.

The slower decay component τ_{ESA} is attributed to excited state lifetime. In both samples it directly corresponds to literature values for fluorescence lifetime of 0.95–1.3 ns [29–32]. The slight decrease of the excited state lifetime in PMMA could originate from contaminations or quenching by the polymer.

The faster time constant τ_{rot} is attributed to the decay of the polarization grating and is due to the rotational dephasing of the transition dipole of the solute molecules. Since the transition dipole of *p*-terphenyl is parallel to the major axis [33], only rotation perpendicular to this axis will contribute to the decay of the polarization anisotropy. The two corresponding degrees of freedom have the same geometry, therefore a single exponential decay of τ_{rot} is expected in the liquid solution as confirmed by the experiment.

The rotational dephasing time τ_{rot} can be calculated by the modified Stokes–Einstein–Debye equation [1–5], taking into account the effect of the solute shape:

$$\tau_{\mathrm{R}} = \frac{V\eta}{k_{\mathrm{B}}T} fC + \tau_{\mathrm{fr}} \tag{3}$$

where V is the volume of a solute molecule, η is the viscosity of the solvent, k_{B} is the Boltzmann constant, T is absolute temperature, f is Perrin's correction parameter for the geometry of the solute [4], C is a parameter depending on the hydrodynamic boundary condition ("stick" or "slip") [5] and τ_{fr} is the "free rotor relaxation time" [34] that corresponds to the rotational dephasing time at zero viscosity. For a calculation of V, f and C *p*-terphenyl was assumed to be of prolate ellipsoid shape. The parameter f is then given by

$$f = \frac{2(\rho^2+1)(\rho^2-1)^{3/2}}{3\rho\left[(2\rho^2-1)\ln\{\rho+(\rho^2-1)^{1/2}\} - \rho(\rho^2-1)^{1/2}\right]} \tag{4}$$

where ρ is the ratio of the long to the short axis of the ellipsoid [4]. The calculation of τ_{rot} according to Eqs. (3) and (4) requires knowledge of the geometrical dimensions of *p*-terphenyl which are not straightforward to determine.

According to Bondi [35], the van der Waals volume of *p*-terphenyl amounts to 224 Å^3 while the van der Waals lengths of the long and short axes amount to 15.9 Å and 6.4 Å, respectively. However, axis lengths and van der Waals volume stand in contradiction if *p*-terphenyl is assumed to be of prolate ellipsoid shape, leading to an uncertainty of about $\pm 25\%$ in volume or about $\pm 10\%$ in the axial dimensions. These uncertainties result from the larger volume of an ellipsoid of Bondi's axis lengths and the shorter axis lengths of an ellipsoid of Bondi's volume, respectively. Thus, we took Bondi's above given values for volume and major axis length as fixed and calculated the minor axis length of the corresponding ellipsoid as 4.9 Å, a value 1.5 Å smaller than Bondi's short axis length. As there are hardly any specific, "nonmechanical" interactions present in the nonpolar solute/solvent combination of *p*-terphenyl and cyclohexane, slip boundary condition was assumed. The value of C was determined as 0.46 according to the table by Hu and Zwanzig [5], and τ_{fr} was assumed 2.6 ps [36]. Thus, with a viscosity of cyclohexane of 0.898 mPa s at room temperature [37] from Eqs. (3) and (4) a rotational relaxation time of 57 ps was obtained that corresponds well to our value of (65 ± 12) ps. Literature values for rotational diffusion times of *p*-terphenyl in different alkanes range from 47 to 70 ps [32, 36, 38] at similar viscosities.

On first sight it might be surprising that τ_{rot} of *p*-terphenyl in PMMA does not exceed τ_{rot} in cyclohexane by orders of magnitude in spite of the rigidity of the polymeric matrix. Deviations of τ_{rot} from expected values towards smaller ones are often explained by free volume effects [7, 36, 39, 40]. In the case of PMMA this means that a certain portion of the dopant molecules would be trapped in free volume nanocavities provided by the amorphous polymer film [13–16]. Depending on the relative dimensions of cavity and trapped molecule the chromophore should be able to rotate relatively undisturbed. τ_{rot} should follow a single exponential decay law in our experimental time window, since effects like structural relaxations of the host matrix which lead to a distribution of decay times take place on a many-minute time scale (*e.g.* [8, 9]).

To further verify this, the radius of the assumed spherical nanocavities in the polymer film has to be estimated. This is often done from orthopositronium (o-ps) triplet lifetimes by the use of the semiempirical Tao–Eldrup equation [41, 42]:

$$\tau_3 = \frac{1}{2}\left[1 - \frac{R}{R_0} + \frac{1}{2\pi}\sin\left(\frac{2\pi R}{R_0}\right)\right]^{-1} \tag{5}$$

where τ_3 is the o-ps lifetime in ns, R is the radius of free volume nanocavity, and R_0 is the radius of a finite spherical potential around the cavity with a thick-

ness $\Delta R = R_0 - R$ and an assumed constant electron density inside ΔR. The value of ΔR in molecular solids like plastic crystals has been determined to $\Delta R = 1.656$ Å [43].

By inserting the τ_3 values by Wang *et al.* [44] into Eq. (5) one obtains free volume site radii of (2.7 ± 0.1) Å at room temperature. These radii are about 3 times too small to provide the possibility of quasi-free rotation of *p*-terphenyl with its long axis diameter between 15.9 Å and 13.5 Å, even if neglecting some more recent papers that suggest the Tao-Eldrup model might lead to slightly too large nanocavity volumes [45–47]. However, it is worth to note that the way we prepared the samples is most likely to result in a larger free volume compared to that in the commercial 3 mm PMMA plates used by Wang *et al.* [44]. The relatively slow solvent evaporation from our films is likely to influence the packing density and thus the average free volume cavity size. Therefore, the interpretation of the decay behaviour in PMMA in terms of a free volume effect seems to be justifiable.

Measurements of the orientational relaxation of dopant molecules in polymeric matrices often reveal a certain distribution breadth of decay times which is best fitted by a stretched exponential function (*e.g.* [8, 9]). However, this is only true for long-term behavior of the chromophores when influences on dipole moment orientation like structural relaxations of the polymer matrix come into play which take place on a many-minute time scale. Our experimental setup opens a different time window: it provides ps resolution while on the other hand it is restricted to maximum delay times of about 1.5 ns. Therefore it is insensitive to the abovementioned relatively slow effects while it is suitable for measurements of fast initial relaxation processes.

More detailed information about the reported molecular mobility in nanocavities could be gained by temperature dependent experiments and variations of transient grating and solvent/polymer parameters.

4. Conclusion

In a cyclohexane solution and in a rigid poly(methyl methacrylate) (PMMA) film, *p*-terphenyl shows a biexponential decay with the slower component being attributable to excited state lifetime ($\tau_{2,\mathrm{CHx}} = 1258 \pm 29$ ps, $\tau_{2,\mathrm{PMMA}} = 988 \pm 80$ ps). Both results correspond well to literature values of 0.95 ns–1.3 ns. The slight reduction of τ_{ESA} in PMMA is possibly due to quenching by the polymer. In the case of the liquid solution, the faster component ($\tau_{1,\mathrm{CHx}} = (65 \pm 12)$ ps, $\tau_{1,\mathrm{PMMA}} = (60 \pm 7)$ ps) corresponds well to rotational reorientation times derived from the hydrodynamic Stokes–Einstein–Debye model under slip boundary conditions, whereas in the polymer film it is interpreted in terms of a free volume effect. Temperature dependent measurements and variations of transient grating and solvent/polymer parameters are natural extensions of the work presented here.

Acknowledgement

The authors are grateful to the Deutsche Forschungsgemeinschaft for financial support in the framework of Sonderforschungsbereich 448.

References

1. G. Stokes, Trans. Cambridge Philos. Soc. **9** (1956) 5.
2. A. Einstein, Ann. Phys. Leipzig **19** (1906) 371.
3. P. Debye, *Polar Molecules*. Dover, New York (1928).
4. P. F. Perrin, J. Phys. Rad. **5** (1934) 497.
5. C. Hu and R. Zwanzig, J. Chem. Phys. **60** (1974) 4354.
6. A. Gierer and K. Wirtz, Z. Naturforsch. A **8** (1953) 532.
7. J. L. Dote, D. Kivelson, and R. N. Schwartz, J. Phys. Chem. **85** (1981) 2169.
8. A. P. Bartko, K. Xu, and R. M. Dickson, Phys. Rev. Lett. **89** (2002) art. no. 026 101.
9. L. A. Deschenes and D. A. Vanden Bout, Science **292** (2001) 255.
10. D. B. Hall, A. Dhinojwhala, and J. M. Torkelson, Phys. Rev. Lett. **79** (1997) 103.
11. M. S. Mehata, H. C. Joshi, and H. P. Tripathi, Spectrochim. Acta A **58** (2002) 1589.
12. S. C. Brower and L. M. Hayden, J. Polymer Sci. B **36** (1998) 1013.
13. T. A. Fayed, J. A. Organero, I. Garcia-Ochoa, L. Tormo, and A. Douhal, Chem. Phys. Lett. **364** (2002) 108.
14. I. M. Kalogeras and A. Vassilikou-Dova, J. Phys. Chem. B **105** (2001) 7651.
15. K. Tawa, K. Kamada, T. Sakaguchi, and K. Ohta, Polymer **41** (2000) 3235.
16. L.-Y. Liu, D. Ramkrishna, and H. S. Lackritz, Macromolecules **27** (1994) 5987.
17. A. von Jena and H. E. Lessing, Opt. Quant. Electron. **11** (1979) 419.
18. A. Henseler and E. Vauthey, Chem. Phys. Lett. **228** (1994) 66.
19. E. Vauthey, Chem. Phys. Lett. **216** (1993) 530.
20. H. J. Eichler, P. Günter, and D. W. Pohl, *Laser Induced Dynamic Gratings*. Springer, Berlin (1986).
21. F. W. Deeg and M. D. Fayer, J. Chem. Phys. **91** (1989) 2269.
22. C. Glorieux, K. A. Nelson, G. Hinze, and M. D. Fayer, J. Chem. Phys. **116** (2002) 3384.
23. R. S. Moog, M. D. Ediger, S. G. Boxer, and M. D. Fayer, J. Phys. Chem. **86** (1982) 4694.
24. R. Menzel and P. Witte, Chem. Phys. Lett. **142** (1987) 366.
25. R. Menzel, *Laser Jahrbuch*, 2nd edition. Vulkan-Verlag, Essen, Germany (1990), p. 223
26. R. Sander, V. Herrmann, and R. Menzel, J. Chem. Phys. **104** (1996) 4390.
27. A. B. Myers and R. Hochstrasser, IEEE J. Quant. Electron. **22** (1986) 1482.
28. I. B. Berlman, *Handbook of Fluorescence Spectra of Aromatic Molecules*. Academic Press, New York (1965).
29. H. Kogelnik, Bell Sys. Tech. J. **48** (1969) 2909.
30. C. D. Amata, M. Burton, W. P. Helman, P. K. Ludwig, and S. A. Rodemeyer, J. Chem. Phys. **48** (1968) 2374.
31. H. Lami, G. Pfeffer, and G. Laustriat, J. Physique **27** (1966) 398.
32. N. Ito, O. Kajimoto, and K. Hara, Chem. Phys. Lett. **318** (2000) 118.
33. I. Baraldi, M. C. Bruni, and F. Momicchioli, Chem. Phys. Lett. **11** (1971) 368.
34. D. R. Bauer, J. I. Brauman, and R. Pecora, J. Am. Chem. Soc. **96** (1974) 6840.
35. A. Bondi, J. Phys. Chem. **68** (1964) 441.
36. J. Benzler and K. Luther, Chem. Phys. Lett. **279** (1997) 333.
37. *CRC Handbook of Chemistry and Physics*, 83rd edn. CRC press, Boca Raton, London (2002).

38. L. A. Philips, S. P. Webb, and J. H. Clark, J. Chem. Phys. **83** (1985) 5810.
39. S. Canonica, A. A. Schmid, and U. P. Wild, Chem. Phys. Lett. **122** (1985) 529.
40. M. Roy and S. Doraiswamy, J. Chem. Phys. **98** (1992) 3213.
41. S. J. Tao, J. Chem. Phys. **56** (1972) 5499.
42. M. Eldrup, D. Lightbody, and J. N. Sherwood, Chem. Phys. **63** (1981) 51.
43. H. Nakanishi and Y. C. Jean, *Positrons and Positronium in Liquids*. In: D. M. Schrader, Y. C. Yean (Eds.): *Positron and Positronium Chemistry*, vol. 57. Elsevier, Amsterdam (1988), p. 159.
44. C. L. Wang, T. Hirade, and F. H. J. Maurer, J. Chem. Phys. **108** (1998) 4654.
45. T. Goworek, Chem. Phys. Lett. **366** (2002) 184.
46. J. Kansy, G. Consolati, and C. Dauwe, Rad. Phys. Chem. **58** (2000) 427.
47. J. Kansy, T. Suzuki, T. Ogawa, and M. Murakami, Rad. Phys. Chem. **58** (2000) 545.